



CHORUS

This is the accepted manuscript made available via CHORUS. The article has been published as:

Nonlinear Quantum Optomechanics via Individual Intrinsic Two-Level Defects

Tomás Ramos, Vivishek Sudhir, Kai Stannigel, Peter Zoller, and Tobias J. Kippenberg

Phys. Rev. Lett. **110**, 193602 — Published 9 May 2013

DOI: [10.1103/PhysRevLett.110.193602](https://doi.org/10.1103/PhysRevLett.110.193602)

Nonlinear Quantum Optomechanics via Individual Intrinsic Two-Level Defects

Tomás Ramos,^{1,2} Vivishek Sudhir,³ Kai Stannigel,^{1,2} Peter Zoller,^{1,2} and Tobias J. Kippenberg³

¹*Institute for Theoretical Physics, University of Innsbruck, 6020 Innsbruck, Austria*

²*Institute for Quantum Optics and Quantum Information of the Austrian Academy of Sciences, 6020 Innsbruck, Austria*

³*École Polytechnique Fédérale de Lausanne (EPFL), 1015 CH, Lausanne, Switzerland*

We propose to use the intrinsic two-level system (TLS) defect states found naturally in integrated optomechanical devices for exploring cavity QED-like phenomena with localized phonons. The Jaynes-Cummings-type interaction between TLS and mechanics can reach the strong coupling regime for existing nano-optomechanical systems, observable via clear signatures in the optomechanical output spectrum. These signatures persist even at finite temperature, and we derive an explicit expression for the temperature at which they vanish. Further, the ability to drive the defect with a microwave field allows for realization of phonon blockade, and the available controls are sufficient to deterministically prepare non-classical states of the mechanical resonator.

Introduction.— Cavity optomechanics [1–3] has enabled the preparation of mechanical resonators in states of low phonon occupation via optomechanical (OM) sideband cooling [4–9], and to observe their quantum coherent interaction with light [9]. Further, OM systems have enabled displacement detection at or even below the standard quantum limit [10–12], thereby complementing other mechanics-based sensing applications [13, 14]. They have also been proposed for creating macroscopic quantum superpositions [15] as well as for applications in quantum information [16, 17]. However, in experiments carried out so far, the interaction between mechanical oscillator and cavity field is effectively linear, while one of the major challenges in the field is to realize non-linearities at the single phonon level. For example, the intrinsic OM radiation pressure non-linearity is predicted to enable the generation of non-classical states of light and mechanics [18, 19], provided that the single-photon coupling rate exceeds the mechanical frequency and the cavity decay rate. In multi-mode OM systems, the same non-linearity can be exploited more easily and it has been proposed to use it for enhanced readout [20] and quantum information processing [21].

Here we propose an alternative route to render the dynamics of the mechanical oscillator nonlinear at the single quantum level: using its natural coupling to intrinsic structural two-level system (TLS) defects and thereby alleviating the need to functionalize the system [see Fig. 1(a)]. Ensembles of TLS defects were first studied in the context of the anomalous and universal low temperature properties of glasses [22–26], where they arise from frustration. In experiments involving Josephson junctions, individual TLSs with transition energies distributed well into the GHz regime were observed and studied for their role in decoherence [27]. Nevertheless, their comparatively long coherence times, and their ability to strongly couple to Josephson junctions via the electric dipole moment have enabled a TLS quantum memory [28]. In the same context, the influence of strain on TLSs has been probed recently [29]. However, in the OM setting, TLS ensembles have mainly been studied

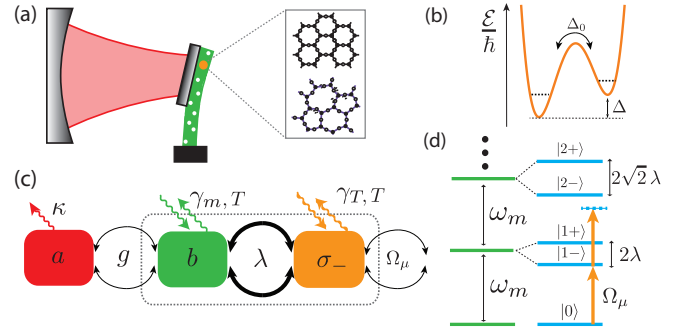


FIG. 1. (a) Strain-coupling of a single two-level system (TLS) defect to an optomechanical system. (b) At low temperature, the defect can be effectively described by two states in a double-well potential, where Δ_0 is the tunnel splitting frequency and Δ the asymmetry frequency. (c) Schematic illustration of decay channels and couplings (see text). Resonator and TLS form a Jaynes-Cummings model (dashed box), exhibiting the characteristic anharmonic spectrum shown in (d).

as a source of decoherence [30–32]. In this letter, we demonstrate theoretically that the coupling of an individual TLS to a localized phonon mode of an OM system can be large enough to exceed the mechanical and TLS dissipation rates, and hence it provides a route to cavity QED-like experiments with single phonons. Such experiments have recently been proposed using a different class of defect states, consisting of donor-acceptor impurity doped silicon [33, 34]. The interaction between TLS and OM system is shown below to be described by a Jaynes-Cummings (JC) Hamiltonian [31, 35], induces single-phonon nonlinearities that can be witnessed in the OM cavity output spectrum. Additionally driving the TLS with microwaves leads to phonon blockade, entailing a mechanical state with sub-Poissonian statistics; and more complex mechanical states can be engineered using suitable protocols. Beyond this, our results also apply to other classes of defect states [33, 34, 36], and OM experiments with single defects may mature our yet incomplete understanding of TLSs in glasses [37].

Strong coupling between resonator and TLS.— We con-

sider OM systems made of silica, where intrinsic TLSs exist due to the amorphous nature of the material, or silicon, where TLS defects reside in the amorphous native (or artificially grown) oxide of the silicon surface [38]. OM systems can be described by an optical cavity mode a coupled to a co-localized deformational mode b of frequency ω_m , with the Hamiltonian including the intrinsic TLS given by

$$H = H_{\text{om}} + H_{\text{JC}} + H_{\text{TLS},\mu}. \quad (1)$$

Here, $H_{\text{om}} = -\hbar\Delta_L a^\dagger a + \hbar g(a + a^\dagger)(b + b^\dagger)$ describes the standard linearized OM coupling of rate g in a frame rotating at the frequency of the driving laser ω_L , which is detuned from the bare cavity resonance by Δ_L [1, 2]. The remaining terms contain the interactions of the mechanical mode with the TLS and the microwave drive of the TLS, as introduced below.

Defects in low-temperature glasses are effectively described by TLSs with tunnel splitting $\hbar\Delta_0$ and asymmetry energy $\hbar\Delta$ [24], such that the eigenstates are split by $\Delta_T = \sqrt{\Delta^2 + \Delta_0^2}$ [see Fig. 1(b)]. Since Δ depends on the strain in the material, the TLS in the OM system couples to the localized phonon mode b [24, 31]. The latter produces a zero-point strain fluctuation on the order of $S_{\text{zpf}} = (\hbar\omega_m/2EV_m)^{1/2}$, where E is the Young's modulus of the material and the mechanical mode volume V_m is defined in analogy to optical cavity QED as [39]

$$V_m = \frac{\int T_{ij}(\mathbf{x})S_{ij}(\mathbf{x})d^3\mathbf{x}}{ES_{ij}(\mathbf{x}_0)S_{ij}(\mathbf{x}_0)}. \quad (2)$$

Here, T_{ij} and S_{ij} are the tensorial stress and strain profiles, respectively, and repeated indices are summed over. Further, \mathbf{x}_0 denotes the point where $S_{ij}S_{ij}$ becomes maximal. Denoting by σ_i the Pauli matrices in the TLS eigenbasis, the interaction between resonator and TLS can be approximated by the JC Hamiltonian $H_{\text{JC}} = (\hbar\Delta_T/2)\sigma_z + \hbar\omega_m b^\dagger b + \hbar\lambda(\sigma_+ b + \sigma_- b^\dagger)$, provided that $\lambda \ll \Delta_T \approx \omega_m$ [35]. Here, the TLS-phonon coupling λ is given by [39]

$$\lambda \approx \frac{D_T}{\hbar} \frac{\Delta_0}{\Delta_T} \left(\frac{\hbar\omega_m}{2EV_m} \right)^{1/2}, \quad (3)$$

where D_T is the deformation potential [40, 41] and we have neglected factors on the order of one due to the exact position and orientation of the TLS.

In addition to strain, the TLS is also susceptible to classical electromagnetic fields [24, 42]. It responds to a coherent microwave drive of Rabi-frequency Ω_μ according to $H_{\text{TLS},\mu} = \hbar\Omega_\mu e^{i\omega_\mu t}\sigma_- + \hbar\Omega_\mu^* e^{-i\omega_\mu t}\sigma_+$. On the other hand, a static electric field \mathbf{E}_0 causes a change in the asymmetry, $\delta\Delta = 2\mathbf{p} \cdot \mathbf{E}_0/\hbar$, where \mathbf{p} is the dipole moment of the TLS, and thereby changes the splitting by $\delta\Delta_T = 2(\Delta/\Delta_T)\mathbf{p} \cdot \mathbf{E}_0/\hbar$ and the coupling by a smaller amount $\delta\lambda = -2\lambda(\Delta/\Delta_T^2)\mathbf{p} \cdot \mathbf{E}_0/\hbar$. Also in the case of artificial donor-acceptor based systems [34], similar tuning

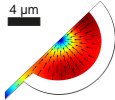
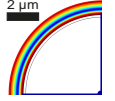
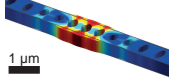
Mechanical mode profile	$\omega_m/2\pi$ [GHz]	V_m [μm^3]	$\lambda_{\text{max}}/2\pi$ [MHz]	N_T
	0.46	13.46	0.13	0.93
	1.34	1.32	0.55	0.26
	5.0	0.01	10.76	0.08

TABLE I. Finite-element simulations of mechanical mode profiles for a radial breathing mode of a silica microsphere [43], a pinch mode of a Si spoke-anchored microdisc [44], and a localized breathing mode of a Si photonic crystal nanobeam [7] (from top to bottom). Here λ_{max} is calculated using Eq. (3) with $D_T = 1.4\text{eV}$ [40], $\Delta_0 = \Delta_T$, and well-known material properties [45]. $N_T \approx 0.8\hbar\lambda_{\text{max}}V_T\bar{P}$ denotes the number of relevant TLSs in a volume V_T [39], i.e. those within a bandwidth λ around ω_m that have $\Delta_0/\Delta_T \gtrsim 0.7$. $\bar{P} = 10^{45}\text{J}^{-1}\text{m}^{-3}$ is the spectral density [31]. For amorphous silica V_T equals the mode volume V_m , whereas for silicon, V_T corresponds to the relevant volume of the amorphous native oxide layer [38].

can be afforded by external electric and magnetic fields.

In Table I we display the results of full finite-element simulations of the mechanical modes of three different OM structures. In addition to ω_m , V_m and $\lambda \propto \sqrt{\omega_m/V_m}$, we also show the number N_T of TLSs that couple resonantly and appreciably to the mechanical mode. While $N_T \lesssim 1$ is desirable in order not to couple to several TLSs, a value of $N_T \ll 1$ can be compensated by the above-mentioned tunability, which allows shifting an off-resonant TLS into resonance with the mechanical mode. In particular, already moderate electric fields $|\mathbf{E}_0| \sim 10^3\text{V/m}$ allow for shifts of $\delta\Delta_T/2\pi \sim 1\text{MHz}$, where we used $|\mathbf{p}| \sim 0.5\text{D}$ [42] and $\Delta_0/\Delta_T \sim 0.9$. The TLS-phonon couplings λ estimated in Table I clearly exceed the typical cryogenic mechanical linewidth $\gamma_m/2\pi \sim 10\text{kHz}$ realized in recent experiments [7, 9]. On the other hand, typical TLS relaxation rates $\gamma_T/2\pi$ have been measured to be in the range 0.1–5 MHz for GHz frequencies [40, 46], and experiments suggest that they dominate over dephasing rates [46], which we thus ignore in this work. Using the bulk value $\gamma_T/2\pi \sim 1\text{MHz}$ at $T \sim 1\text{K}$ [24], we obtain $\lambda/\gamma_T \sim 10$ for the case of the nanobeam. The phonon density of states responsible for TLS relaxation is strongly suppressed in the proposed structures as compared to the bulk, which leads us to consider these numbers a worst-case estimate.

We conclude from the above discussion and the results

in Table I that strong coupling to individual defects is feasible for suitably engineered OM systems. While the couplings in the microsphere and microdisc structures are on the verge of the strong coupling regime, the most promising structure is the nanobeam. In the following, we derive the signatures of the TLS-resonator interaction in the OM output spectrum and show that the coupling enables quantum state control of the mechanical resonator in analogy to atomic cavity QED.

Optomechanical output spectrum.— In the absence of the microwave drive ($\Omega_\mu = 0$), the system is only driven by thermal and vacuum fluctuations, as described by the master equation

$$\dot{\rho} = -\frac{i}{\hbar}[H, \rho] + \mathcal{L}_c \rho + \mathcal{L}_m \rho + \mathcal{L}_T \rho, \quad (4)$$

with Lindblad terms $\mathcal{L}_c \rho = \kappa \mathcal{D}[a] \rho$ for the cavity, and

$$\mathcal{L}_T \rho = \gamma_T (\bar{n}_T + 1) \mathcal{D}[\sigma_-] \rho + \gamma_T \bar{n}_T \mathcal{D}[\sigma_+] \rho, \quad (5)$$

$$\mathcal{L}_m \rho = \gamma_m (\bar{n}_m + 1) \mathcal{D}[b] \rho + \gamma_m \bar{n}_m \mathcal{D}[b^\dagger] \rho, \quad (6)$$

for TLS and resonator, respectively [see also Fig. 1(c)]. Here, κ is the cavity energy decay rate, $\bar{n}_{m,T}$ are the Bose occupation numbers corresponding to an environment at temperature T and $\mathcal{D}[x] \rho \equiv x \rho x^\dagger - (x^\dagger x \rho + \rho x^\dagger x)/2$. We consider the case where the three systems are in resonance ($-\Delta_L \approx \omega_m \approx \Delta_T$), and where the cavity adiabatically follows the resonator dynamics [$\kappa \gg g, \gamma_T(\bar{n}_T + 1), \gamma_m(\bar{n}_m + 1)$]. In this regime, the OM coupling leads to cooling of the mechanical resonator and the TLS [35]: For the case $\lambda \ll \kappa$ of relevance in this work, the optically induced mechanical damping rate $A^{(-)} \approx 4g^2/\kappa$ can exceed the corresponding heating rate $A^{(+)} \approx g^2\kappa/4\omega_m^2$, as well as the rethermalization rate $\gamma_m \bar{n}_m$. In addition, the OM coupling transduces the resonator motion to the cavity output, and thereby enables the observation of the hybridized resonator-TLS subsystem by photodetection. In particular, we consider here the cavity output spectrum $S(\omega) = (\kappa/2\pi) \int_{-\infty}^{\infty} d\tau e^{-i(\omega - \omega_L)\tau} \langle a^\dagger(\tau) a(0) \rangle_{ss}$, where the angular brackets denote the average in the steady state of Eq. (4).

In Figure 2 we display $S(\omega)$ for frequencies around the blue sideband $\omega_{\text{blue}} \equiv \omega_L + \omega_m$ as a function of temperature. The spectra show transitions between the levels of the JC Hamiltonian H_{JC} formed by resonator and TLS [dashed box in Fig. 1(c)]. In the case of exact resonance ($\omega_m = \Delta_T$), the ground state energy of H_{JC} is zero and the excited states $|n\pm\rangle$ have energies $\omega_{n\pm} = n\omega_m \pm \lambda\sqrt{n}$ ($n = 1, 2, \dots$), giving rise to the ‘‘JC ladder’’ shown in Fig. 1(d). For $T \rightarrow 0$ almost all population is in the lowest states of the ladder, such that only the transitions at $\omega = \omega_{\text{blue}} \pm \lambda$ between the first rung and the ground state are observed. As temperature increases, higher states get populated, so that transitions between higher rungs located at $\omega = \omega_L + \omega_{n\alpha\beta}$, with $\omega_{n\alpha\beta} \equiv \omega_{n\alpha} - \omega_{(n-1)\beta}$ ($\alpha, \beta = \pm$), also become visible

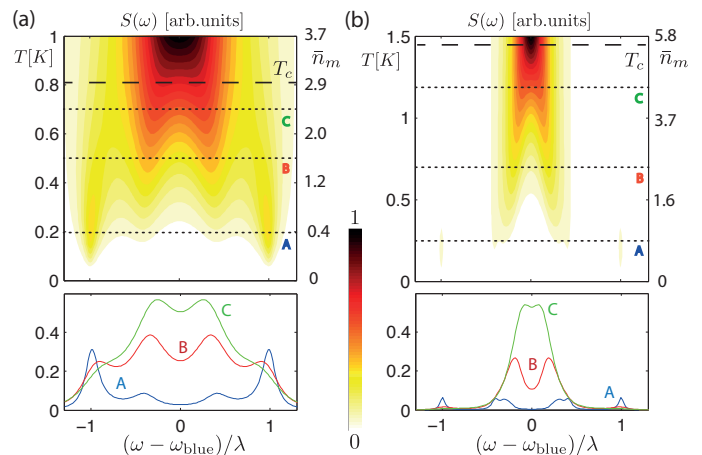


FIG. 2. Fine-structure of the OM output spectrum $S(\omega)$ around the blue sideband at ω_{blue} as a function of temperature and without a microwave drive field ($\Omega_\mu = 0$). The dashed line shows the cross-over temperature according to Eq. (8) and the lower panels show cross sections at the temperatures indicated by dotted lines in the top panels. Parameters are $\omega_m = 2\pi \cdot 5$ GHz, $\kappa = 0.1\omega_m$, $\lambda = 2 \cdot 10^{-3}\omega_m$, $\gamma_m = 6 \cdot 10^{-6}\omega_m$ and (a) $g = \lambda$, $\gamma_T = \lambda/10$, (b) $g = \lambda/10$, $\gamma_T = \lambda/30$.

in the output spectrum. Finally, above a certain cross-over temperature T_c the spectrum consists of a single Lorentzian peak, since the upper and lower branches of the JC ladder resemble two independent highly excited harmonic oscillators [47]. Note that below T_c , temperature actually helps to observe transitions between higher rungs in the JC ladder.

To estimate T_c , we adiabatically eliminate the cavity mode and calculate $S(\omega)$ using a secular approximation, which is valid as long as the individual spectral lines do not overlap [48]. The resulting blue sideband of $S(\omega)$ can be approximated by a sum over Lorentzians $l_\omega(\omega_0, \gamma_0) = \gamma_0^2 / (\gamma_0^2 + (\omega - \omega_L - \omega_0)^2)$ [39], i.e.,

$$S_{\text{blue}}(\omega) \approx \sum_{n=1}^{\infty} \sum_{\alpha, \beta=\pm} W_{n\alpha\beta}^{\text{blue}} l_\omega(\omega_{n\alpha\beta}, \gamma_{n\alpha\beta}/2), \quad (7)$$

where each term corresponds to a transition $|n\alpha\rangle \rightarrow |(n-1)\beta\rangle$ centered at $\omega = \omega_L + \omega_{n\alpha\beta}$. Since $\lambda \ll \kappa$, the widths can be written as $\gamma_{n\alpha\beta} = 2(n-1)\bar{\gamma}(\bar{n}+1) + 2n\bar{\gamma}\bar{n} + \gamma_T(2\bar{n}_m+1)$, for $n \geq 2$, and $\gamma_{1\alpha+} = \bar{\gamma}(3\bar{n}+1/2) + \gamma_T(2\bar{n}_m+1/2)$. Here, $\bar{\gamma} = \gamma_m + A^{(-)} - A^{(+)}$ is the effective mechanical damping rate and $\bar{n} = (\bar{n}_m\gamma_m + A^{(+)})/\bar{\gamma}$ the corresponding effective mean occupation, as known from standard OM cooling [4, 5]. The weights in Eq. (7) are expressed in general as $W_{n\alpha\beta}^{\text{blue}} \equiv (2A^{(-)} p_{n\alpha} B_{n\alpha\beta}^2) / (\pi\gamma_{n\alpha\beta})$, where $p_{n\alpha}$ is the steady state population of the eigenstate $|n\alpha\rangle$. The JC matrix elements read $B_{n\alpha\beta}^2 = (2n-1 + 2\alpha\beta\sqrt{n(n-1)})/4$, for $n \geq 2$, and $B_{1\alpha+}^2 = 1/2$.

As temperature increases and population moves up the JC ladder, transitions between the \pm -branches become irrelevant, while the ones within each branch occur closer

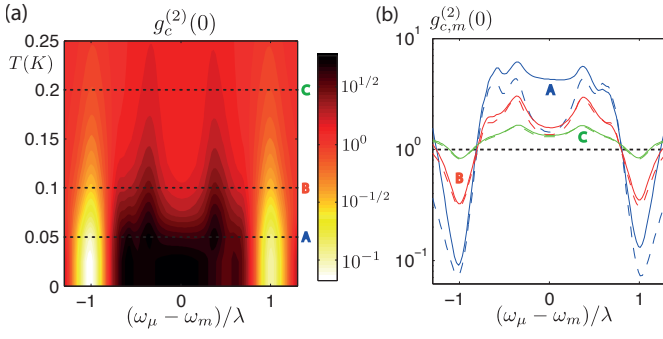


FIG. 3. Optically probed phonon blockade. (a) $g_c^{(2)}(0)$ of the cavity as a function of drive frequency ω_μ and temperature T for $|\Omega_\mu| = 0.1\lambda$. All other parameters as in Fig. 2(a). (b) $g_c^{(2)}(0)$ of the cavity (solid) at temperatures indicated by dashed lines in panel (a), and corresponding $g_m^{(2)}(0)$ of the resonator (dashed).

to $\omega = \omega_{\text{blue}}$ and thus contribute to the center of the spectrum. We define the cross-over point as the temperature T_c where the separation of the two dominant Lorentzians in Eq. (7) (at each side of $\omega = \omega_{\text{blue}}$) equals their width, i.e., where $2\lambda(\sqrt{N} - \sqrt{N-1}) \approx \gamma_{N++}$, with N being the index n for which W_{n++}^{blue} is maximal. If we further restrict the parameters to a regime of experimental interest: $A^{(+)} \ll \gamma_m \bar{n}_m^c \ll A^{(-)} \lesssim \gamma_T \ll \lambda$ and $\bar{n}_m^c \gg 1$, where \bar{n}_m^c is the bath mean occupation at T_c , then the cross-over criterion yields [39]:

$$T_c \approx \frac{\hbar\omega_m}{k_B} \bar{n}_m^c \approx \frac{\hbar\omega_m}{k_B} \left(\frac{\lambda}{2\gamma_T} \right)^{2/3} \frac{(1 + 2A^{(-)}/\gamma_T)}{(1 + 3A^{(-)}/\gamma_T)^{2/3}}. \quad (8)$$

Naturally, T_c increases with increasing coupling λ and decreases when increasing the TLS linewidth, but additionally Eq. (8) shows that T_c can be increased by enhancing the OM cooling rate $A^{(-)}$. The above estimate for T_c agrees well with our numerical simulations, as can be seen from Fig. 2 (dashed lines). For finite detuning $|\omega_m - \Delta_T| \lesssim \lambda$ of TLS and mechanics the general picture described above remains valid, although the spectra generally become asymmetric.

Optically probed phonon blockade.— By driving the TLS with a weak coherent microwave field ($|\Omega_\mu| \ll \lambda$) we can realize a phonon blockade in analogy to cavity QED [49]: if the JC system is cooled to its ground state and the drive is tuned to a transition $|0\rangle \rightarrow |1\pm\rangle$, then the subsequent transition $|1\pm\rangle \rightarrow |2\pm\rangle$ is suppressed provided that $\lambda \gg \gamma_T$, see Fig. 1(d). The resulting sub-Poissonian resonator statistics ($g_m^{(2)}(0) \equiv \langle b^\dagger b^\dagger b b \rangle / \langle b^\dagger b \rangle^2 < 1$) persist at finite T if $\exp(-\hbar\omega_m/k_B T) \ll |\Omega_\mu|^2/\gamma_{\pm\pm}^2$, which ensures that the thermal occupation is irrelevant compared to the one due to the drive. Since the cavity operator adiabatically follows the mechanics, i.e. $a(t) \approx -2ig/\kappa[b(t) - i(\kappa/4\omega_m)b^\dagger(t)] + \text{noise}$ [39], we have that $g_m^{(2)}(0) \approx g_c^{(2)}(0) \equiv \langle a^\dagger a^\dagger a a \rangle / \langle a^\dagger a \rangle^2$ to zeroth order in

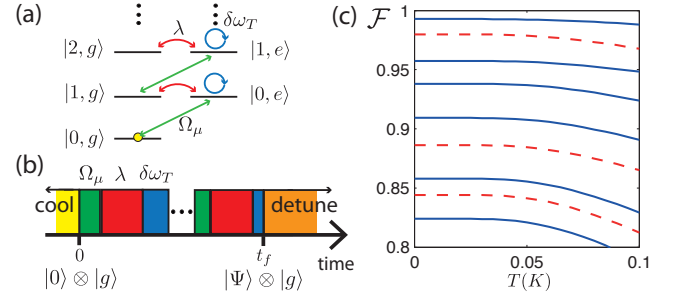


FIG. 4. Preparation of non-classical resonator states based on Ref. [50]. (a) Level scheme with available tools and (b) general sequence for preparation of a resonator arbitrary state $|\Psi\rangle$ using OM cooling, strong TLS drive ($|\Omega_\mu| \gg \lambda$), free evolution ($\sim \lambda$), strong TLS AC-Stark shift $\delta\omega_T \sim |\Omega_\mu|^2/|\omega_\mu - \Delta_T| \gg \lambda$, and TLS-resonator detuning. (c) Fidelity $\mathcal{F} = \langle \Psi_M | \rho(t_f) | \Psi_M \rangle$ as a function of temperature and for increasing M from top to bottom. Dashed curves: $M = 1, 2, 3$ and parameters as in Fig. 2(a). Solid curves: $M = 1, 2, 3, 4, 7, 9$ and parameters as before, except for $\gamma_T = \lambda/30$. The OM interaction is switched off after the initial cooling.

$\kappa/\omega_m \ll 1$, such that the phonon blockade can be probed optically. Figure 3(a) displays $g_c^{(2)}(0)$ of the cavity as a function of drive frequency and temperature. For low T , one clearly observes the expected anti-bunching at $\omega_\mu = \omega_m \pm \lambda$, while these features disappear for higher T due to thermal occupation of the JC ladder. As can be seen from the cuts presented in Fig. 3(b), the $g^{(2)}(0)$ -function of the cavity is an upper bound for the one of the resonator in the region of pronounced anti-bunching and therefore, an optical $g_c^{(2)}(0) < 1$ indicates phonon blockade.

Preparation of non-classical states.— The possibility to electrically tune and coherently drive the TLS, together with the strong coherent coupling between TLS and resonator gives rise to the prospect of deterministically preparing quantum states by suitable protocols. As an example, we propose preparing the system close to its ground state by OM cooling and then generating a non-classical resonator state by a scheme analogous to the one of Ref. [50]. The necessary sequence is illustrated in Figs. 4(a,b), and as an example we plot in Fig. 4(c) the resulting fidelities for preparing the states $|\Psi_M\rangle \equiv (|0\rangle + |M\rangle)/\sqrt{2}$ ($M = 1, 2, \dots$), in the presence of imperfections. Clearly, the fidelity decreases with increasing M and T . However, already for $\lambda/\gamma_T = 10$ one can achieve $\mathcal{F} > 0.95$ for temperatures around 100mK, which constitutes an exciting avenue for OM systems in existence today.

Acknowledgments.— Work in Innsbruck was supported by the Austrian Science Fund (FWF) through SFB FOCUS and by the EU network AQUITE. T.R. further acknowledges financial support from the BECAS CHILE scholarship program. V.S. and T.J.K. are supported by

the ERC starting grant SiMP and the NCCR QSIT program of the Swiss National Science Foundation.

-
- [1] T. J. Kippenberg and K. J. Vahala, *Science* **321**, 1172 (2008).
- [2] F. Marquardt and S. M. Girvin, *Physics* **2**, 40 (2009).
- [3] G. J. Milburn and M. J. Woolley, *Acta Physica Slovaca* **61**, 483 (2011).
- [4] F. Marquardt, J. P. Chen, A. A. Clerk, and S. M. Girvin, *Phys. Rev. Lett.* **99**, 093902 (2007).
- [5] I. Wilson-Rae, N. Nooshi, W. Zwerger, and T. J. Kippenberg, *Phys. Rev. Lett.* **99**, 093901 (2007).
- [6] A. O’Connell, M. Hofheinz, M. Ansmann, R. Bialczak, M. Lenander, E. Lucero, M. Neeley, D. Sank, H. Wang, M. Weides, J. Wenner, J. Martinis, and A. Cleland, *Nature* **464**, 697 (2010).
- [7] J. Chan, T. P. M. Alegre, A. H. Safavi-Naeini, J. T. Hill, A. Krause, S. Gröblacher, M. Aspelmeyer, and O. Painter, *Nature* **478**, 89 (2011).
- [8] J. Teufel, T. Donner, D. Li, J. Harlow, M. Allsman, K. Cicak, A. Sirois, J. Whittaker, K. Lehnert, and R. Simmonds, *Nature* **475**, 359 (2011).
- [9] E. Verhagen, S. Deleglise, S. Weis, A. Schliesser, and T. J. Kippenberg, *Nature* **482**, 63 (2012).
- [10] J. Teufel, T. Donner, M. Castellanos-Beltran, J. Harlow, and K. Lehnert, *Nature Nanotech.* **4**, 820 (2009).
- [11] G. Anetsberger, O. Arcizet, Q. Unterreithmeier, R. Riviere, A. Schliesser, E. Weig, M. Gorodetsky, J. Kotthaus, and T. J. Kippenberg, *Nature Physics* **5**, 909 (2009).
- [12] T. Westphal, D. Friedrich, H. Kaufer, K. Yamamoto, S. Gossler, H. Müller-Eberhardt, S. Danilishin, F. Khalili, K. Danzmann, and R. Schnabel, *Phys. Rev. A* **85**, 063806 (2012).
- [13] A. Naik, M. Hanay, W. Hiebert, X. Feng, and M. Roukes, *Nature Nanotech.* **4**, 445 (2009).
- [14] E. Gavartin, P. Verlot, and T. J. Kippenberg, *Nature Nanotech.* **7**, 509 (2012).
- [15] W. Marshall, C. Simon, R. Penrose, and D. Bouwmeester, *Phys. Rev. Lett.* **91**, 130401 (2003).
- [16] J. Zhang, K. Peng, and S. L. Braunstein, *Phys. Rev. A* **68**, 013808 (2003).
- [17] K. Stannigel, P. Rabl, A. S. Sorensen, P. Zoller, and M. D. Lukin, *Phys. Rev. Lett.* **105**, 220501 (2010).
- [18] A. Nunnenkamp, K. Borkje, and S. Girvin, *Phys. Rev. Lett.* **107**, 063602 (2011).
- [19] P. Rabl, *Phys. Rev. Lett.* **107**, 063601 (2011).
- [20] M. Ludwig, A. H. Safavi-Naeini, O. Painter, and F. Marquardt, *Phys. Rev. Lett.* **109**, 063601 (2012).
- [21] K. Stannigel, P. Komar, S. J. M. Habraken, S. D. Bennett, M. D. Lukin, P. Zoller, and P. Rabl, *Phys. Rev. Lett.* **109**, 013603 (2012).
- [22] R. C. Zeller and R. O. Pohl, *Phys. Rev. B* **4**, 2029 (1971).
- [23] P. W. Anderson, B. I. Halperin, and C. M. Varma, *Phil. Mag.* **25**, 1 (1972).
- [24] W. A. Phillips, *Rep. Prog. Phys.* **50**, 1657 (1987).
- [25] A. Heuer and R. J. Silbey, *Phys. Rev. Lett.* **70**, 3911 (1993).
- [26] C. Enss and S. Hunklinger, *Low-Temperature Physics* (Springer-Verlag Berlin Heidelberg, 2005).
- [27] J. M. Martinis, K. B. Cooper, R. McDermott, M. Steffen, M. Ansmann, K. D. Osborn, K. Cicak, S. Oh, D. P. Pappas, R. W. Simmonds, and C. C. Yu, *Phys. Rev. Lett.* **95**, 210503 (2005).
- [28] M. Neeley, M. Ansmann, R. C. Bialczak, M. Hofheinz, N. Katz, E. Lucero, A. O’Connell, H. Wang, A. N. Cleland, and J. M. Martinis, *Nature Physics* **4**, 523 (2008).
- [29] G. Grabovskij, T. Peichl, J. Leisenfeld, G. Weiss, and A. Ustinov, *Science* **338**, 232 (2012).
- [30] C. Seoáñez, F. Guinea, and A. H. Castro Neto, *Phys. Rev. B* **77**, 125107 (2008).
- [31] L. G. Remus, M. P. Blencowe, and Y. Tanaka, *Phys. Rev. B* **80**, 174103 (2009).
- [32] R. Rivière, S. Deléglise, S. Weis, E. Gavartin, O. Arcizet, A. Schliesser, and T. J. Kippenberg, *Phys. Rev. A* **83**, 063835 (2011).
- [33] O. O. Soykal, R. Ruskov, and C. Tahan, *Phys. Rev. Lett.* **107**, 235502 (2011).
- [34] R. Ruskov and C. Tahan, *arXiv:1208.1776* (2012).
- [35] L. Tian, *Phys. Rev. B* **84**, 035417 (2011).
- [36] S. D. Bennett, N. Y. Yao, J. Otterbach, P. Zoller, P. Rabl, and M. D. Lukin, *Phys. Rev. Lett.* **110**, 156402 (2013).
- [37] K. Agarwal, I. Martin, M. D. Lukin, and E. Demler, *Phys. Rev. B* **87**, 144201 (2013).
- [38] M. Morita, T. Ohmi, E. Hasegawa, M. Kawakami, and M. Ohwada, *J. Appl. Phys.* **68**, 1272 (1990).
- [39] See supplemental information for details.
- [40] B. Golding and J. E. Graebner, *Phys. Rev. Lett.* **37**, 852 (1976).
- [41] D. V. Anghel, T. Kühn, Y. M. Galperin, and M. Manninen, *Phys. Rev. B* **75**, 064202 (2007).
- [42] H. M. Carruzzo, E. R. Grannan, and C. C. Yu, *Phys. Rev. B* **50**, 6685 (1994).
- [43] D. W. Vernooy, V. S. Ilchenko, H. Mabuchi, E. W. Streed, and H. J. Kimble, *Opt. Lett.* **23**, 247 (1998).
- [44] C. Xiong, X. Sun, K. Y. Fong, and H. X. Tang, *Appl. Phys. Lett.* **100**, 171111 (2012).
- [45] M. Poot and H. S. van der Zant, *Physics Reports* **511**, 273 (2012).
- [46] J. Lisenfeld, C. Müller, J. H. Cole, P. Bushev, A. Lukashenko, A. Shnirman, and A. V. Ustinov, *Phys. Rev. Lett.* **105**, 230504 (2010).
- [47] J. M. Fink, L. Steffen, P. Studer, L. S. Bishop, M. Baur, R. Bianchetti, D. Bozyigit, C. Lang, S. Filipp, P. J. Leek, and A. Wallraff, *Phys. Rev. Lett.* **105**, 163601 (2010).
- [48] L. Tian and H. J. Carmichael, *Quantum Opt.* **4**, 131 (1992).
- [49] K. Birnbaum, A. Boca, R. Miller, A. Boozer, T. Northrup, and H. Kimble, *Nature* **436**, 87 (2005).
- [50] C. K. Law and J. H. Eberly, *Phys. Rev. Lett.* **76**, 1055 (1996).